CHEMISTRY
A EUROPEAN JOURNAL

DOI: 10.1002/chem.201002061

The Electron Localizability Indicator from X-Ray Diffraction Data—A First Application to a Series of Epoxide Derivatives

Simon Grabowsky,*[a] Dylan Jayatilaka,[b] Stefan Mebs,[a] and Peter Luger[a]

The description of electron pairs is at the heart of understanding the chemistry of a given compound because reorganization of electron pairs drives any chemical reaction. A widely used method to describe the electron distribution within a compound is the topological analysis of the electron density (ED).[1] The ED gives information on concentration and depletion of electrons, but not on the pairing of electrons. In contrast, the recently introduced electron localizability indicator (ELI[2]) is a measure of electron pair localization. Up to now, a great advantage of the ED over the ELI was that only the ED could be derived from a crystallographic X-ray diffraction experiment. Herein, we describe how we made the ELI deducible from the experiment by using the X-ray constrained wavefunction (XCW) fitting procedure.[3] In this method, a wavefunction for an isolated molecule or one embedded in the crystal is constrained to reproduce the X-ray diffraction data while minimizing the electronic energy. We implemented the formula of the ELI (ELI-D(t),[4]) into the program Tonto[5] and thus made it accessible to the experimentally derived wavefunction resulting from the XCW fitting procedure.[6]

Epoxide derivatives serve as test cases for a first application of the new experimentally derived ELI. The high strain in the three-membered C-O-C ring causes broad synthetic[7] and pharmaceutical[8] applications of epoxides. Molecular orbital models describe the two main aspects of the ring strain: The Förster–Coulson–Moffitt model[9] shows that C–O and C–C bonds are bent outwards, whereas the Walsh model[10] shows delocalization through the interior of the ring. Both imply that the epoxide ring is unsaturated and can interact with π systems. For cyclopropane, experimental ED studies confirm that bonds bend outwards;[11] but for epoxides, there are only few experimental ED studies with inconclusive results.[12] In this work, a series of epoxide derivatives is studied. From unsubstituted epoxide (**1**) to tetracyanoepoxide (**4**), the number and strength of electron-withdrawing substituents increase continuously. Compounds **3** and **4** serve as model compounds for pharmaceutically important protease inhibitors.[13]

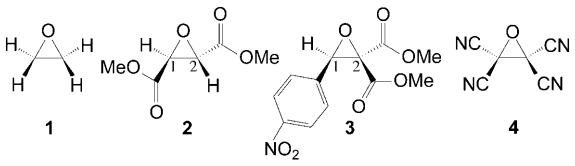

Single crystals were obtained and measured at low temperatures (25 and 100 K) and up to very high resolutions ($d < 0.5$ Å) mainly using a synchrotron source.[14] The final geometries and the experimentally derived ED distributions were determined by multipole modeling.[15] Subsequent XCW fitting yielded experimentally derived wavefunctions (HF/cc-pVDZ), from which the ELI was calculated and topologically analyzed (model *exp*). For comparison, isolated-molecule calculations were performed at the experimental (model *sp*) and at the optimized (model *opt*) geometries at the same level of theory. For experimental and computational details, see the Supporting Information.

The representations of the topology of the epoxide ring in Figure 1 are generally the same for all four compounds and for the three models, *exp*, *sp*, and *opt*, detailed differences will be discussed below. Valence-shell charge concentrations (VSCCs, Figure 1a) in the Laplacian for C–C and C–O bonds are shifted outwards the bond axes, which indicates outwardly bent bonds. But in contrast, the C–O bond critical points (bcps, Figure 1b) are located exactly on the bond

[a] Dr. S. Grabowsky, Dr. S. Mebs, Prof. Dr. P. Luger
Freie Universität Berlin
Institut für Chemie und Biochemie/Anorganische Chemie
Fabeckstr. 36a, 14195 Berlin (Germany)
Fax: (+49) 30-838-53464
E-mail: vongrabo@chemie.fu-berlin.de

[b] Prof. D. Jayatilaka
The University of Western Australia, School of Biomedical
Biomolecular & Chemical Sciences, 35 Stirling Highway
Crawley WA 6009 (Australia)

Supporting information for this article is available on the WWW under http://dx.doi.org/10.1002/chem.201002061.

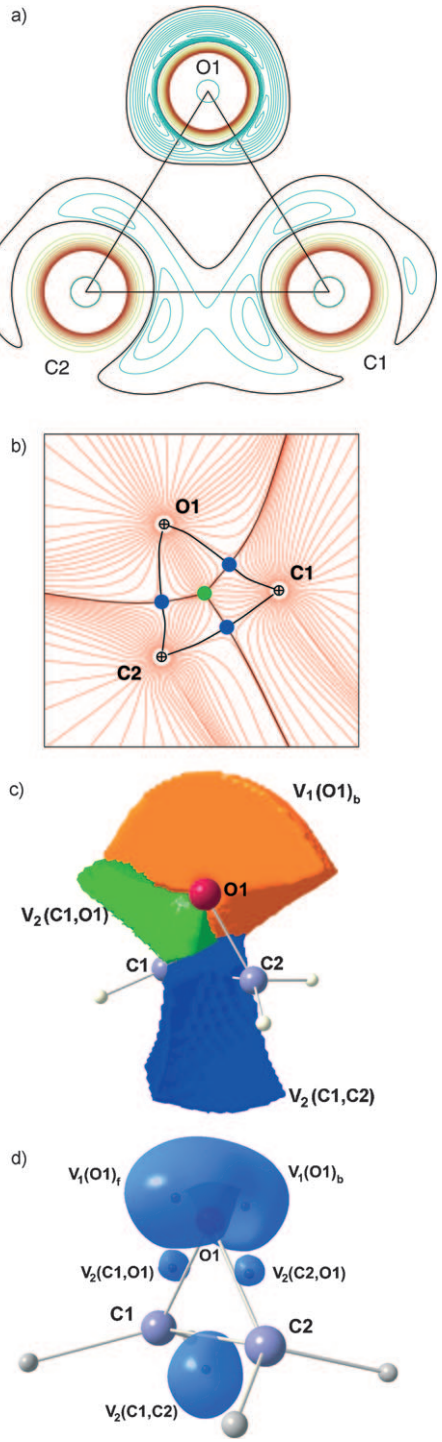

Figure 1. ED and ELI representations of the epoxide ring displaying the general topology for all compounds and models. Disynaptic valence basin of the C–C bond: V_2(C1,C2); disynaptic valence basins of the C–O bonds: V_2(C,O1); monosynaptic valence basins of the foremost/backmost oxygen lone pairs: $V_1(O1)_{fb}$. a) Experimental Laplacian map of the ED, contour interval = 7 e Å^{-5} (blue = negative, red = positive, black = zero) for **4**. b) Experimental gradient vector field and molecular graph with critical points (cps) (blue = bond cps, green = ring cp) for **1**. c) Shapes of three representative valence basins, outer contour cut at $\rho = 0.001$ a.u. = 0.0067 e Å^{-3}, optimized geometry of **1**. d) Experimental localization domain representation with attractor positions visible under the transparent isosurfaces (isovalue = 1.45) for **4**.

axes; strain is expressed in an S-type shape of the C–O bond paths. So for both C–C and C–O bonds, the bond paths are about 0.01 to 0.02 Å longer than the bond axes. Due to this ambiguous description of bond character in the ED, it is indispensable to examine the localization of the electron pairs forming the bonds. Figure 1c shows the shapes of valence basins in the epoxide ring. Corresponding localization domains (regions of highest localization of the electron pairs) and the attractors of the basins (absolute maxima of the ELI distribution) are depicted in Figure 1d. They are clearly shifted outwards for both the C–C and C–O bond axes, so that the localization of the electron pairs constituting the bonds is in accordance with the Förster–Coulson–Moffitt model.

The localization domain representations of the experimentally derived ELI for all compounds are given in Figures 2a–d. Typical and expected cashew-nut-like shapes of

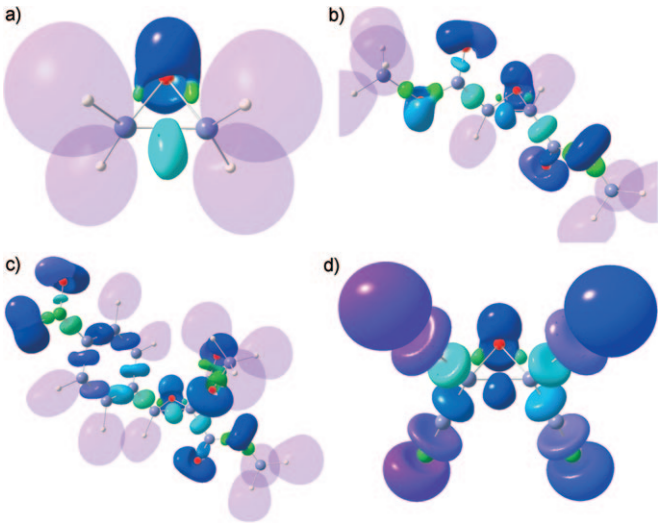

Figure 2. Experimental ELI localization domain representations, protonated monosynaptic valence basins for H atoms in transparent mode. Color code makes domains belonging to different basins distinguishable from each other; MolIso[16] graphics. a) **1**, isovalue = 1.41. b) **2**, isovalue = 1.45. c) **3**, isovalue = 1.45. d) **4**, isovalue = 1.45.

oxygen lone pairs, toroidal shapes of the valence basins of the cyano groups (**4**), or prolated shapes of 1.5-fold bonds in the phenyl group (**3**) are visible. The C–O bond domains in the epoxide ring are remarkably small, compare, for example, the C–O bonds in the ester groups of **2** and **3**.

The electron populations of the bonds and lone pairs in the epoxide ring with corresponding ELI values at the attractors are summarized in Table 1. Three major conclusions can be drawn:

1) Ring strain: Corresponding to the small bond domains, the electron populations of the C–O bonds are remarkably low, too. Each electron pair constituting a C–O bond contains only around 1.0 e, except for **1** in model *exp*, where the value is about 0.6 e due to crystal effects (see

Table 1. Comparison of experimentally and theoretically derived ELI-D populations ELI_{pop} (e) and values at the attractors ELI_{att} (without dimension) for valence basins in the epoxide rings of **1** to **4**. [Experiment (*exp*) as well as isolated molecule calculations at experimental (*sp*) and optimized geometry (*opt*); a detailed table with individual values for both C–O bonds and oxygen lone pairs is given in the Supporting Information.]

Basin	Method	**1**	**2**	**3**	**4**
sum of both	ELI_{pop} *exp*	1.16	1.95	1.98	2.04
V_2(C,O1)	ELI_{pop} *sp*	2.03	2.11	2.18	2.25
	ELI_{pop} *opt*	2.19	2.24	2.29	2.38
average of both	ELI_{att} *exp*	1.454	1.514	1.523	1.539
V_2(C,O1)	ELI_{att} *sp*	1.461	1.521	1.532	1.533
	ELI_{att} *opt*	1.482	1.531	1.543	1.550
V_2(C1,C2)	ELI_{pop} *exp*	1.82	1.85	1.87	1.84
	ELI_{pop} *sp*	1.91	1.88	1.90	1.86
	ELI_{pop} *opt*	1.87	1.86	1.90	1.88
	ELI_{att} *exp*	1.903	1.960	1.887	1.901
	ELI_{att} *sp*	1.891	1.898	1.916	1.913
	ELI_{att} *opt*	1.886	1.892	1.924	1.936
sum of both	ELI_{pop} *exp*	5.94	5.34	5.30	5.29
V_1(O1)	ELI_{pop} *sp*	5.35	5.29	5.25	5.22
	ELI_{pop} *opt*	5.22	5.18	5.17	5.11
average of both	ELI_{att} *exp*	1.749	1.812	1.812	1.823
V_1(O1)	ELI_{att} *sp*	1.737	1.798	1.801	1.809
	ELI_{att} *opt*	1.730	1.789	1.793	1.797
sum of all	ELI_{pop} *exp*	8.92	9.14	9.15	9.17
populations	ELI_{pop} *sp*	9.29	9.28	9.33	9.33
	ELI_{pop} *opt*	9.28	9.28	9.36	9.37

point 2 below). C–C bonds are populated with 1.8–1.9 e, which is still significantly lower than the value of 2.0 e commonly found for a normal C–O or C–C single bond. The low populations of the bonds are only partly compensated for by the unusually high populations of the oxygen lone pairs (the sum of all populations is significantly smaller than 10 e), so that the strained and unsaturated character of the epoxide ring is reflected in the populations.

2) Crystal effects: Comparing the results in the sequence *exp*→*sp*→*opt*, the influence of crystal effects on the ELI values can be quantified. For the C–C bonds, no trend is visible; but the C–O bonds and the oxygen lone pairs are influenced by the crystal environment in a regular and consistent manner. C–O bond populations are lowest in model *exp* and increase towards model *opt*. Consequently, the opposite is true for the populations of the oxygen lone pairs, which are correspondingly highest in model *exp* and decrease towards model *opt*. The ELI values at the attractors show the same trend. The extremely low C–O bond population and the extremely high population of the oxygen lone pairs of **1** in the experiment are due to the fact that intermolecular interactions are most important in the crystal lattice of **1**. It is the only one of the four compounds in which the epoxide oxygen atom serves as acceptor for hydrogen bonds.[12] Hence, the experimentally derived ELI gives essential information if intermolecular interactions become dominant. This can also be seen in the sums of all populations inside the ring: The experimentally derived populations (*exp*) on the one hand are lower than the theoretically derived ones (*sp* and *opt*) on the other hand, but the effect is strongest for **1**.
3) Substituent effects: With increasing number and strength of electron-withdrawing substituents from **1** towards **4**, the C–O bond populations increase and the populations of the oxygen lone pairs decrease. In contrast, the ELI values at the attractors of both C–O bonds and oxygen lone pairs are smallest for **1** and increase steadily towards **4**. This means that each electron pair in the epoxide ring is more localized with increasing number and strength of electron-withdrawing substituents. Localization of electron pairs is therefore not necessarily connected to the electron number of electron pairs, but gives complementary information that cannot be obtained, for example, by the ELF.[6] Moreover, crystal and substituent effects reflected in the ELI properties cannot be found for ED and Laplacian values at corresponding bcps (see the Supporting Information).

In this work, we have introduced the ELI based on an X-ray diffraction experiment by means of the X-ray constrained wavefunction fitting procedure. As a first application, the electronic nature of the epoxide ring could be enlightened: The ELI clearly indicates outwardly bent bonds according to the Förster–Coulson–Moffitt model, which could not be derived unambiguously from the ED. Substituent and crystal effects could be separated from each other for a series of acceptor-substituted epoxide derivatives and the importance of the experimentally derived ELI was demonstrated. It is a property that makes the detailed description of electron pairs accessible to experimental chemists, who think in terms of electron pairs and energy. So it is intended in the future to combine the experimentally derived ELI with energetical components through the XCW approach and extend it towards the description of reaction processes.

Keywords: bond theory · electron density · electron localizability indicator · epoxides · X-ray diffraction

[1] a) R. F. W. Bader, *Atoms in Molecules: A Quantum Theory*, 1st ed., no. 22 in The International Series of Monographs on Chemistry, Clarendon Press, Oxford, **1990**; b) R. F. W. Bader, P. L. A. Popelier, T. A. Keith, *Angew. Chem.* **1994**, *106*, 647–659; *Angew. Chem. Int. Ed. Engl.* **1994**, *33*, 620–631; c) P. Coppens, *Angew. Chem.* **2005**, *117*, 6970–6972; *Angew. Chem. Int. Ed.* **2005**, *44*, 6810–6811; d) T. S. Koritsánszky, P. Coppens, *Chem. Rev.* **2001**, *101*, 1583–1628.
[2] M. Kohout, *Int. J. Quantum Chem.* **2004**, *97*, 651–658.
[3] a) D. Jayatilaka, D. J. Grimwood, *Acta Crystallogr. Sect. A* **2001**, *57*, 76–86; b) D. J. Grimwood, D. Jayatilaka, *Acta Crystallogr. Sect. A* **2001**, *57*, 87–100.
[4] The ELI-D(t) is the widest used variant of the ELI. A fixed fraction (D) of a same-spin electron pair coupling to a triplet (t) state is used for its derivation; a) M. Kohout, *Faraday Discuss.* **2007**, *135*, 43–54; b) F. R. Wagner, V. Bezugly, M. Kohout, Y. Grin, *Chem. Eur. J.* **2007**, *13*, 5724–5741.
[5] D. Jayatilaka, D. J. Grimwood, *Computational Science - ICCS 2003, Part 4, Chapter Tonto: A Fortran Based Object-Oriented System for*

Quantum Chemistry and Crystallography, Springer, Berlin, **2003**, 142–151. To be downloaded free of charge under: http://tonto-chem.sourceforge.net.

[6] The electron localization function (ELF), the precursor of the ELI, is already deducible from an XCW (D. Jayatilaka, D. J. Grimwood, *Acta Crystallogr. Sect. A* **2004**, *60*, 111–119). But as the ELF is not a measure of electron pair localization, but a relative property, it is indispensable to use the ELI to analyze electron pairing.

[7] A. Padwa, S. S. Murphree, *ARKIVOC* **2006**, *3*, 6–33.

[8] a) J. C. Powers, J. L. Asgian, Ö. D. Ekici, K. E. James, *Chem. Rev.* **2002**, *102*, 4639–4750; b) E. Martina, N. Stiefl, B. Degel, F. Schulz, A. Breuning, M. Schiller, R. Vicik, K. Baumann, J. Ziebuhr, T. Schirmeister, *Bioorg. Med. Chem. Lett.* **2005**, *15*, 5365–5369.

[9] C. A. Coulson, T. H. Goodwin, *J. Chem. Soc.* **1962**, 2851–2854.

[10] A. D. Walsh, *Nature* **1947**, *159*, 712–713.

[11] a) T. Koritsánszky, J. Buschmann, P. Luger, *J. Phys. Chem.* **1996**, *100*, 10547–10553; b) P. Luger, M. Messerschmidt, S. Scheins, A. Wagner, *Acta Crystallogr. Sect. A* **2004**, *60*, 390–396.

[12] a) C. L. Klein, E. D. Stevens, *Acta Crystallogr. Sect. A* **1988**, *44*, 50–55; b) S. Grabowsky, M. Weber, J. Buschmann, P. Luger, *Acta Crystallogr. Sect. B* **2008**, *64*, 397–400.

[13] a) S. Grabowsky, T. Pfeuffer, L. Chęcińska, M. Weber, W. Morgenroth, P. Luger, T. Schirmeister, *Eur. J. Org. Chem.* **2007**, 2759–2768; b) S. Grabowsky, T. Pfeuffer, W. Morgenroth, C. Paulmann, T. Schirmeister, P. Luger, *Org. Biomol. Chem.* **2008**, *6*, 2295–2307.

[14] Compounds **2** to **4** were synthesized by Dr. Thomas Pfeuffer in the group of Prof. Dr. Tanja Schirmeister (University of Würzburg, Germany). Synchrotron beamline F1 of the HAYLAB at DESY (Hamburg, Germany) was employed under the supervision of Dr. Carsten Paulmann for **3** and **4**; for **1** and **2**, the in-house diffractometer was used. Details on the crystal structure analysis are given in the Supporting Information.

[15] N. K. Hansen, P. Coppens, *Acta Crystallogr. Sect. A* **1978**, *34*, 909–921.

[16] C. B. Hübschle, P. Luger, *J. Appl. Crystallogr.* **2006**, *39*, 901–904. To be downloaded free of charge under: http://www.moliso.de.

Received: July 20, 2010
Published online: September 30, 2010

